Annals of Biomedical Engineering (© 2015)
DOI: 10.1007/s10439-015-1320-9

Roles of the Fibrous Superficial Zone in the Mechanical Behavior of TMJ Condylar Cartilage

LEONARDO RUGGIERO,[1,2] BRANDON K. ZIMMERMAN,[1] MIRI PARK,[1] LIN HAN,[3] LIYUN WANG,[1] DAVID L. BURRIS,[1] and X. LUCAS LU[1]

[1]Department of Mechanical Engineering, University of Delaware, 130 Academy Street, Newark, DE 19716, USA; [2]Department of Mechanics of Materials and Constructions, Vrije Universiteit Brussel, Brussels, Belgium; and [3]School of Biomedical Engineering, Science & Health Systems, Drexel University, Philadelphia, PA, USA

(*Received 5 February 2015; accepted 7 April 2015*)

Associate Editor Eric M. Darling oversaw the review of this article.

Abstract—In temporomandibular joints (TMJs), the cartilage on the condylar head displays a unique ultrastructure with a dense layer of type I collagen in the superficial zone, different from hyaline cartilage in other joints. This study aims to elucidate the roles of this fibrous zone in the mechanical behaviors, particularly lubrication, of TMJ under physiological loading regimes. Mechanical tests on porcine condylar cartilage demonstrated that the superficial and middle-deep zones exhibit tension–compression nonlinearity. The tensile and compressive moduli of the superficial zone are 30.73 ± 12.97 and 0.028 ± 0.016 MPa, respectively, while those for the middle-deep zone are 2.43 ± 1.75 and 0.14 ± 0.09 MPa. A nonlinear finite element model of condylar cartilage was built to simulate sliding of a spherical probe over the articular surface. The presence of the superficial zone significantly promoted interstitial fluid pressurization (IFP) inside the loaded cartilage and reduced the friction force on the surface, compared to the case without the superficial zone. Finite element simulations showed that IFP depends on sliding speed but not normal load, which matches the experimental results. This study revealed the presence of the fibrous zone can significantly reduce the deformation of condylar cartilage under compression and the friction force on its surface during sliding.

Keywords—Tension–compression nonlinearity, Heterogeneous, Friction coefficient, Interstitial fluid pressurization, Finite element model, Biphasic theory.

Address correspondence to X. Lucas Lu, Department of Mechanical Engineering, University of Delaware, 130 Academy Street, Newark, DE 19716, USA. Electronic mail: xlu@udel.edu

Leonardo Ruggiero and Brandon K. Zimmerman have contributed equally to the work.

INTRODUCTION

The temporomandibular joint (TMJ), consisting of a fibrocartilaginous disc separating the two opposing articular surfaces of the glenoid fossa and mandibular condyle, is the only moving joint in the human head and is subjected to a combination of rotational and translational motion during physiological functions.[19] The primary function of the TMJ is to facilitate mandibular motion by distributing loads, reducing peak stresses, and enabling low-friction movement during daily activities, such as chewing and talking. Although lubrication is crucial for the extended use of TMJ over a lifetime,[30,44] the frictional properties of TMJ cartilaginous tissues have not been studied as extensively as those of regular hyaline cartilage. Using a custom-designed pendulum device, the friction coefficient of an intact TMJ has been reported to be ~0.018, increasing with loading duration, a pattern that is compatible with those of other human diarthrodial joints.[20,42,43]

A number of theoretical[2,27,33] and experimental studies[6,7,14,15,21,32,38] have demonstrated that interstitial fluid pressurization (IFP) is a critical lubrication mechanism in hyaline articular cartilage. In hyaline cartilage, the fluid pressure often supports over 95% of the mechanical loading under physiological conditions, minimizing the load borne by solid–solid contact. As the friction between fluid–fluid and fluid–solid contacts is so low as to be negligible, the resulting friction force on the solid matrix, primarily due to solid–solid contact, is significantly reduced.[2,28] It is believed that IFP, also termed as 'weeping' or 'biphasic' lubrication,[12,20,23] contributes to the excellent lubrication characteristics of diarthrodial joints. In our recent

Published online: 17 April 2015

study, the frictional properties of TMJ disc and condylar cartilage were measured and compared under a physiologically-relevant, migrating contact area (MCA) modality.[48] The friction coefficient of the TMJ condyle was found to be significantly lower than that of the disc, despite the disc's uniform fiber alignment and smooth surface. Examination of the dependency of friction coefficient on Peclet number ($Pe = Vh/H_A k$, V = sliding speed, h = tissue thickness, H_A = aggregate modulus, k = hydraulic permeability) suggested that IFP should play an essential role in the lubrication of TMJ condylar cartilage.

Despite employing IFP for lubrication, as do typical cartilaginous tissues, TMJ condylar cartilage has a unique ultrastructure which is drastically different from that of normal hyaline cartilage. Besides the three hyaline-like proliferative, mature, and hypertrophic zones, termed the 'middle-deep zone' in this study, condylar cartilage possesses an extra fibrous superficial layer (Fig. 1). Large type I collagen bundles can be visually observed in this layer, running tangent to the articular surface and rooting vertically into the middle-deep zone. The superficial layer contains mainly type I collagen with little proteoglycans. In normal hyaline cartilage, the tension–compression nonlinearity of the collagen network is critical to induce and maintain the high fluid pressure in loaded cartilage, and the peak fluid load support ratio is directly related to the ratio between tensile and compressive moduli.[22,27,39] It is natural to conjecture that the presence of the superficial fibrous layer in TMJ condylar cartilage could also regulate the fluid pressure in the loaded tissue and consequently affect joint lubrication. However, few studies have investigated the roles of this unique fibrous zone in the mechanical functions of TMJ condylar cartilage.

In this study, we hypothesize that the existence of the superficial fibrous zone and its tension–compression nonlinearity promotes and maintains IFP in loaded TMJ condylar cartilage, thus benefitting lubrication at the articular surface. To test this hypothesis, we aim to: (1) determine the tensile and compressive moduli of the superficial and middle-deep zones of TMJ condylar cartilage; (2) use finite element (FE) simulations to test the effect of the superficial zone on IFP and lubrication of TMJ condylar cartilage; and (3) test the validity of the simulation results using tribology measurements.

MATERIALS AND METHODS

Porcine TMJ Samples and Friction Tests

Healthy TMJs were harvested from both sides of fresh porcine heads (Green Village, NJ) within 24 h of euthanasia. The animals were of mixed breed and gender, with an average age of 4 months and an average weight of 90 kg. 15 total joints from 9 separate porcine heads were obtained. Any joints displaying signs of wear or damage on disc or condyle were excluded. Left and right joints were pooled together and were not paired for analysis. Porcine TMJ was chosen due to its structural and functional similarities to human TMJ.[5,10] During harvesting, the inferior TMJ capsule was carefully preserved with the disc attached atop the condylar head. Samples were frozen at −80 °C before testing. To examine the ultrastructure and distribution of collagen and proteoglycan across the depth of the tissue, histological images of condylar cartilage, including Sirius red and Safranin O staining, were obtained from the central region of a healthy condyle (Figs. 1b and 1c).

On the day of friction testing, the disc was removed to expose the condylar head, the surface of which was gently washed with phosphate buffered saline (PBS) solution to remove unbound synovial fluid. The sample was balanced in PBS supplemented with a protease inhibitor cocktail for a half hour,[25] then affixed on a

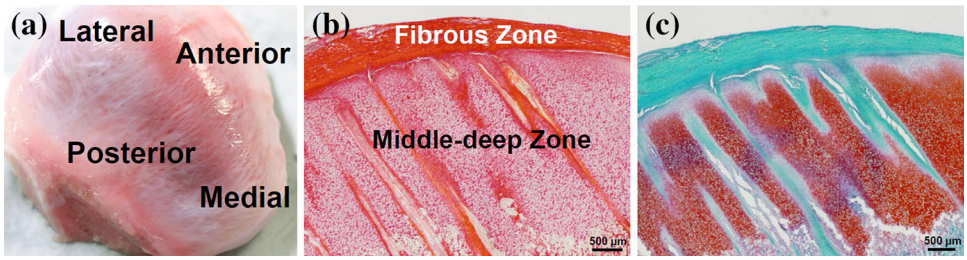

FIGURE 1. Morphology and ultrastructure of porcine TMJ condylar cartilage. (a) Surface of a left mandibular condyle with visible large white collagen bundles aligning predominantly in the anterior–posterior direction. (b) Condylar cartilage (central region, sagittal plane) stained with Sirius red to visualize the distribution of collagen. The superficial zone appears as a separate dense mat composed of massive collagen fibers covering the hyaline-like middle-deep zone. The hyaline cartilage is interdigitated with large collagen bundles rooting from the fibrous zone. (c) Condylar cartilage stained with Safranin O for proteoglycan content. The fibrous zone contains little proteoglycans compared to the hyaline cartilage in the middle-deep zone. Large collagen bundles running across the middle-deep layer are deficient in GAG and can be seen clearly to root in the superficial zone.

custom-built micro-tribometer for friction coefficient measurements, as described previously[6,7] (Fig. 2a). In brief, the subchondral bone of the condylar head was secured in a fluid chamber attached on a 3D ball head, enabling the tissue surface to be aligned perpendicularly to the loading axis of an impervious spherical probe (diameter $\phi = 6.4$ mm). The probe was fixed at the end of a cantilever beam mounted on a motorized linear stage (M-111.2DG, Physik Instrumente, Germany) controlled by a closed-loop feedback loading system, allowing the probe to compress the articular surface with specified constant normal force. Sliding of the probe over a 1.5 mm track along the articular surface was achieved by another DC motor stage (M-403.1PD, Physik Instrumente, Germany), which supported the 3D ball head, fluid chamber, and condyle. This testing setup resulted in MCA sliding between the probe and the articular surface. The cartilage in the central region of six TMJ condyles ($N = 6$) was tested in the anterior–posterior (AP) sliding direction under six different normal loads (25, 50, 75, 100, 150, and 200 mN) at a constant speed of 2 mm/s, and seven sliding speeds (0.05, 0.1, 0.25, 0.5, 1, 2, and 5 mm/s) under a constant load of 100 mN. The adopted loading magnitudes avoided damaging the tissue (strains $<25\%$)[40] and minimized confounding contributions of plowing forces toward the friction coefficient.[6,31] All friction studies were performed in PBS to mitigate the effect of boundary lubrication from synovial fluid constituents.

Frictional and normal forces on the articular surface were measured by two orthogonal capacitance sensors mounted on the cantilever beam. The friction coefficient was determined as the average of the forward and reverse frictional force at equilibrium divided by twice the normal force, thus avoiding measurement errors due to sample curvature.[8] For the duration of the test, the cartilage surface was continually irrigated with abundant PBS supplemented with protease inhibitors to maintain hydration.

Indentation and Tensile Tests

Condyles from nine fresh joints were utilized for indentation and tensile testing ($N = 9$). To perform indentation tests, a cylindrical cartilage-bone explant from the central region of the condylar head was harvested using a 5 mm biopsy punch. The superficial zone of the cartilage explant, approximately 350 μm in thickness, was separated from the rest of the tissue using a sledge microtome equipped with a freezing stage (Leica SM 2400), following similar protocols described in literature.[18,36] The average thickness of the remaining middle-deep zone was 2.13 ± 0.74 mm. To determine the mechanical properties, indentation creep tests were performed on the superficial zone and the middle-deep zone tissues separately using a custom-built micro-indenter.[24,29] The sample was first affixed in a medium chamber atop a 3D ball head. To test the middle-deep zone, the subchondral bone of the plug was attached to the chamber with cyanoacrylate. To mount the thin superficial layer, a bead of cyanoacrylate was placed on a smooth aluminum block in the chamber and immediately removed with a razor blade. The superficial zone was then placed on the residue, holding the base of the sample firm without stiffening the tissue. The tissue surface was then aligned perpendicular to a porous flat-ended cylindrical indenter tip ($\phi = 1.2$ mm). During testing, a 5 mN preload was applied for 5 min, followed by a 20 mN step load for 1 h or until the creep deformation reached equilibrium.[24,25] The step loading was applied using a piezoelectric actuator (P-602.8SL, Physik Instrumente, Germany).

A 5×13 mm rectangular tissue section was excised from the central region of the condylar head immediately adjacent to the indentation site, with the long axis aligned in the anterior–posterior direction (Fig. 3a). Rectangular strips of the superficial zone and the remaining middle-deep layer were prepared with the aforementioned microtome and a custom-built cutting tool.[18] The final dimension of each strip was 1.5×10 mm, and the actual cross-sectional area of the sample was measured using a noncontact optical laser device.[41] Tensile testing of the cartilage strips was performed using an Instron 5848 Microtester (Instron, Norwood, Massachusetts, USA) equipped with thin-sample grips. Specimen mounting closely followed the procedure of Ref. 36. The tensile loading profile consisted of a 10 s ramp to 2% strain followed by a 10 min relaxation period prior to another 2% strain increase, repeated until sample failure[18] (Figs. 3a and 3b). PBS was dripped on the sample during the test using an irrigation system. At each strain level, the equilibrium stress at the end of the relaxation period was calculated and plotted against the tensile strain, producing a stress–strain curve. The tensile modulus of the tissue was calculated as the slope of the linear portion of the curve (Fig. 3b).

Constitutive Models

According to the ultrastructure of condylar cartilage (Fig. 1), both the superficial and middle-deep zones were modeled as fiber-reinforced biphasic materials in FEBio.[26] A solid mixture consisting of a compressible isotropic neo-Hookean ground matrix and three mutually orthogonal fiber bundles was employed for the solid phase of the superficial layer. The adopted constitutive model displays mechanical behaviors similar to a conewise linear elastic (CLE) material.[22,39] The solid phase of the middle-deep zone, similar to

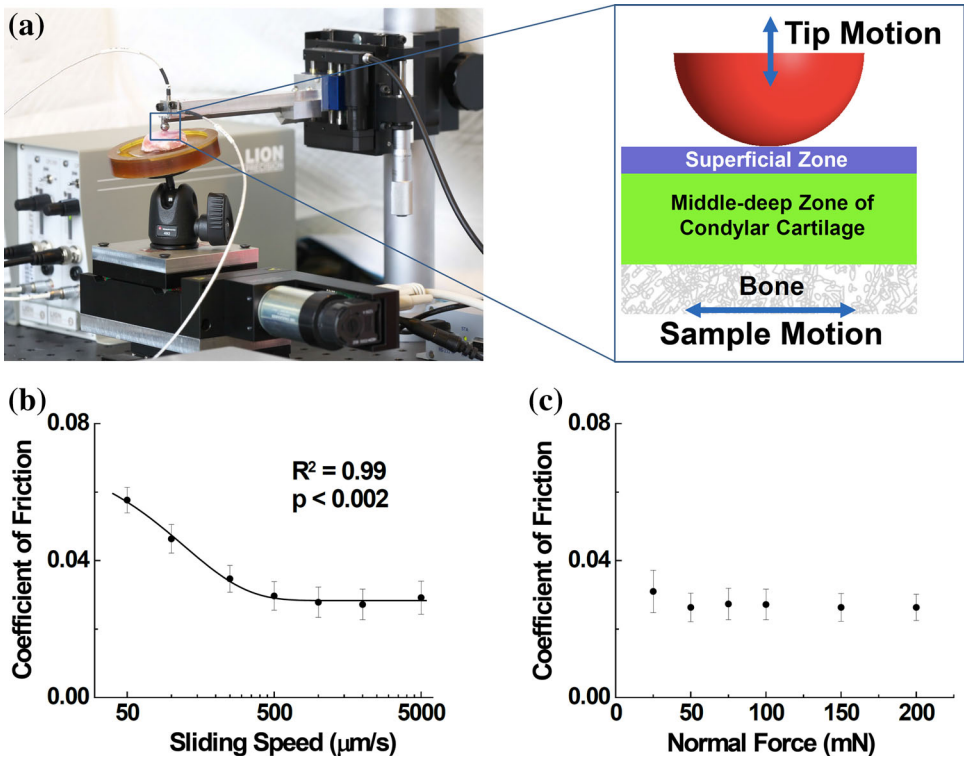

FIGURE 2. Tribology testing of TMJ condylar cartilage. (a) Picture of the custom-built micro-tribometer used for friction measurement. Normal compressive loading is applied by a spherical probe attached to a cantilever beam fixed on the top motorized stage, while sliding of the probe on the cartilage surface is achieved by reciprocation of a linear stage at the bottom. The frictional force and normal force are measured by two capacitance sensors fixed on the tip of the cantilever beam. During testing a PBS drip (not shown) bathes the tissue to ensure adequate hydration. (b) Significant sliding speed dependence of friction coefficient was detected via Spearman's rank correlation coefficient ($p < 0.0001$, normal force kept constant at 100 mN). (c) Friction coefficient displayed no significant dependence on normal compressive force ($p = 0.37$, sliding speed kept constant at 2 mm/s). For both panels, data shown are mean ± SD for $N = 6$ TMJs.

hyaline cartilage in morphology and composition (Figs. 1b, 1c), was modeled as a solid mixture of a neo-Hookean ground material and fibers with a continuous isotropic distribution.[4] Models of both zones incorporated Holmes-Mow strain-dependent permeability for the solid matrix.[17]

Determination of material parameters in both constitutive models was achieved by curve-fitting the experimental creep indentation data obtained from the cartilage explants, with boundary conditions summarized in Fig. 3d. The tensile modulus obtained from tensile tests was used as a known variable during the curve-fitting. Curve-fitting was performed using the bound-constrained Nelder–Mead (NM) algorithm coded in MATLAB (The MathWorks Inc., Natick, Massachusetts, USA). Employment of a derivative-free optimization algorithm (i.e., NM algorithm), bounding of the unknown material parameters to a realistic parameter space, and replication of the iterative procedure with multiple initial guesses were adopted to avoid local minima and non-uniqueness of the solution during curve-fitting.

Simulation of Migrating Contact Sliding

To simulate MCA sliding on the articular surface, a nonlinear heterogeneous FE model was built in FEBio, where the condylar cartilage was modeled as a bilayer material with the proposed constitutive models. The average material properties determined from tensile tests and indentation curve-fitting were used as input into the model (Fig. 4a). An impervious rigid spherical probe ($\phi = 6.4$ mm) compressed the tissue surface with specified strain in 10 s before sliding was initiated along a 1.5 mm wear track on the tissue surface. Ten sliding cycles were simulated to obtain the temporal mechanical responses. Frictionless biphasic contact with an augmented Lagrangian control method was used to simulate the cartilage-probe interaction during sliding and to optimize control of the gap at the contact interface.[3] The other boundary conditions are summarized in Fig. 4b. A symmetric 3D model was used to minimize the number of elements. The element mesh was biased in order to properly capture the rapid variation of the fluid pressure near free-draining

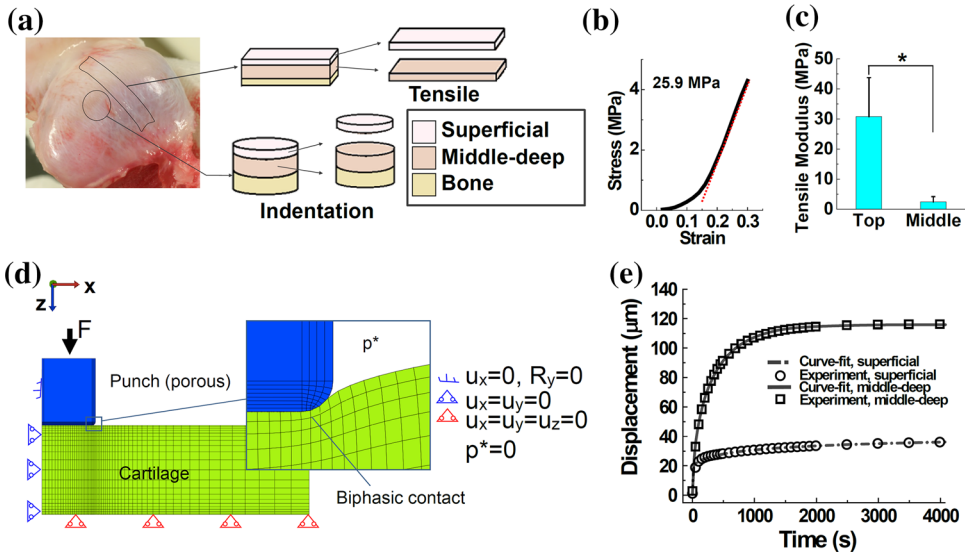

FIGURE 3. Tensile and indentation testing of TMJ condylar cartilage. (a) Schematic depicting the harvest and preparation of samples for mechanical testing. A sledge microtome with freezing stage was used to separate the superficial zone, middle-deep zone, and subchondral bone. (b) A typical stress–strain curve obtained from tensile testing. Slope of the linear region marked by the red line was calculated as the tensile modulus. (c) Tensile moduli for the superficial (top) and middle-deep (middle) zones. The superficial zone displayed a significantly higher tensile modulus than the middle zone ($N = 9$, $p < 0.001$). (d) Boundary conditions and geometry for the simulation of creep indentation in FEBio. Biphasic contact was established between the indenter and the cartilage surface. $U_{x,y,z}$ represents the displacement of the solid matrix, P is fluid pressure, and R_y is the rotation around the y-axis. (e) Typical indentation creep test curves for the superficial and middle-deep zones, with corresponding FE theoretical fittings.

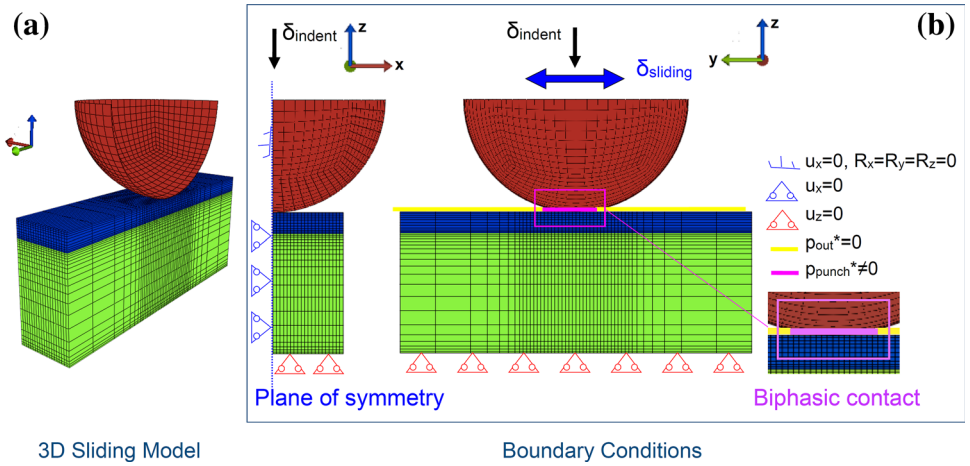

FIGURE 4. Simulation of an impervious rigid spherical probe sliding on TMJ condylar cartilage. (a) Three-dimensional view of the inhomogeneous model. The superficial zone, 15% of the total cartilage thickness, is atop the middle-deep zone. The tissue width was selected such that the contact radius is always less than 25% of the width, to avoid complications from the boundary. Half of the symmetric problem was modeled to save computational time. (b) Boundary conditions for the 3D sliding model: rigid probe holding two degrees of freedom in translation (i.e., in compressive and sliding directions) and zero in rotation, with biphasic contact at the probe-cartilage contact area (magenta contour line). Free-draining conditions are applied outside the contact area (yellow contour line).

boundaries. A total of 28,200 hexahedral elements were used in the model, with the value defined following a mesh convergence study.

Simulations were performed to disclose the influence of the superficial zone of condylar cartilage on its mechanical behaviors by modeling condylar cartilage subjected to sliding in the presence or absence of a superficial layer. The effect of loading magnitude and sliding speed on IFP were also investigated. Sliding simulations were performed for probe speeds of 1 and 2 mm/s under 10% compressive strain, and for 10 and 15% compressive strain at 1 mm/s sliding speed. For all loading conditions, articular cartilage was modeled as either a heterogeneous bilayer material

(heterogeneous model) or a homogeneous material consisting of the middle-deep zone only (homogeneous model). The fluid load support ratio W_p/W, defined as the ratio between the integration of the fluid pressure W_p and the total applied contact force W over the contact area,[22] was calculated to represent the level of IFP within the tissue.

Statistical Analysis

Student's t test was performed to compare the average of tensile modulus, compressive modulus, and permeability to detect whether they varied significantly between superficial and middle-deep zones. Spearman's rank correlation coefficient was utilized to examine the dependence of the friction coefficient on speed or normal force. An exponential fitting was performed between the two variables if a significant correlation was detected. Results are reported as mean ± standard deviation unless otherwise noted. In all tests, $p < 0.05$ was deemed statistically significant.

RESULTS

Mechanical Properties

A visual examination reveals large collagen bundles running across the condylar surface in porcine TMJ, principally aligned in the AP direction in the central region (Fig. 1a). Histology images confirm the superficial zone is a dense mat of collagen fibers (Fig. 1b) with little proteoglycan content (Fig. 1c). Unlike normal hyaline cartilage, the middle-deep zone of TMJ cartilage is characterized by the presence of large collagen bundles, some of which display an arcade-like arrangement, clearly visible in the Safranin O image (Fig. 1c).

The average friction coefficient in the central region of the condylar surface was 0.027 ± 0.004 at 2 mm/s sliding speed with 100 mN normal loading. The friction coefficient decreased significantly from 0.057 ± 0.003 to 0.029 ± 0.004 as the sliding speed increased from 0.05 to 5 mm/s (Fig. 2b). Spearman's rank correlation coefficient revealed a strong exponential dependency ($R^2 = 0.99$) of the condyle friction coefficient on sliding speed ($p < 0.0001$). No such dependency or correlation exists for varying normal force ($p = 0.37$). The friction coefficient changed non-significantly from 0.031 ± 0.006 to 0.026 ± 0.004 as the normal load increased from 25 to 200 mN when sliding speed was kept at 2 mm/s (Fig. 2c) ($N = 6$).

The tensile modulus of the superficial zone in the AP direction is 30.73 ± 12.97 MPa, significantly higher than that of the middle-deep zone (2.43 ± 1.75 MPa, $p < 0.001$) (Fig. 3c). The two fiber-reinforced biphasic models fit the experimental indentation creep curves to a high degree of accuracy, with R^2 values of 0.98 ± 0.03 and 0.94 ± 0.03 for the superficial and middle-deep zones, respectively (Fig. 3e). Mechanical properties obtained from the FE curve-fitting for both zones are listed in Table 1. The superficial zone shows a prominent tension–compression nonlinearity, with a ratio of tensile to compressive modulus of approximately 1098:1 ($H_{+A} = 30.73 \pm 12.97$ vs. $H_{-A} = 0.028 \pm 0.016$ MPa). In contrast, the tension–compression nonlinearity of the middle-deep zone is less prominent, at 17.4:1. The middle-deep zone shows a higher compressive modulus (0.14 ± 0.09 vs. 0.028 ± 0.016 MPa, $N = 9$, $p < 0.01$) and no significant difference in permeability compared to the superficial zone (8.43 ± 7.83 × 10^{-15} vs. 3.77 ± 1.46 × 10^{-15} m^4/Ns, $N = 9$, $p = 0.11$).

FE Simulation Results

In the FEBio simulation the fluid pressure and stress and strain fields within the cartilage were calculated under the MCA testing modality. Contour plots depicting fluid pressure and total stresses are plotted (Fig. 5) when the indenter is at the center of the sliding track, for both the initial state (cycle 0) and final state (cycle 10). In the presence of the superficial fibrous zone (heterogeneous model), the magnitude of the fluid pressure and total stress are higher than those in the homogeneous model (Figs. 5a and 5b). Despite the higher total stress, the stress in the solid matrix is lower

TABLE 1. Mechanical properties determined by curve-fitting creep indentation data for superficial and middle-deep zones ($N = 9$).

Superficial zone			
H_{-A} (MPa)	H_{+A} (MPa)	ν	$k \times 10^{15}$ (m^4/Ns)
0.028 ± 0.016	30.73 ± 12.97	0.094 ± 0.080	3.77 ± 1.46
Middle-deep zone			
H_{-A} (MPa)	ξ (MPa)	ν	$k \times 10^{15}$ (m^4/Ns)
0.140 ± 0.086	0.244 ± 0.215	0.047 ± 0.026	8.43 ± 7.83

Tensile modulus H_{+A} for the superficial layer has been directly determined by tensile tests and used as input in the curve-fitting methodology. For the middle-deep zone the tensile stiffness of fibers ξ was determined by curve-fitting with the other material parameters. H_{-A} is the aggregate compressive modulus, ν is Poisson's ratio, and k is hydraulic permeability.

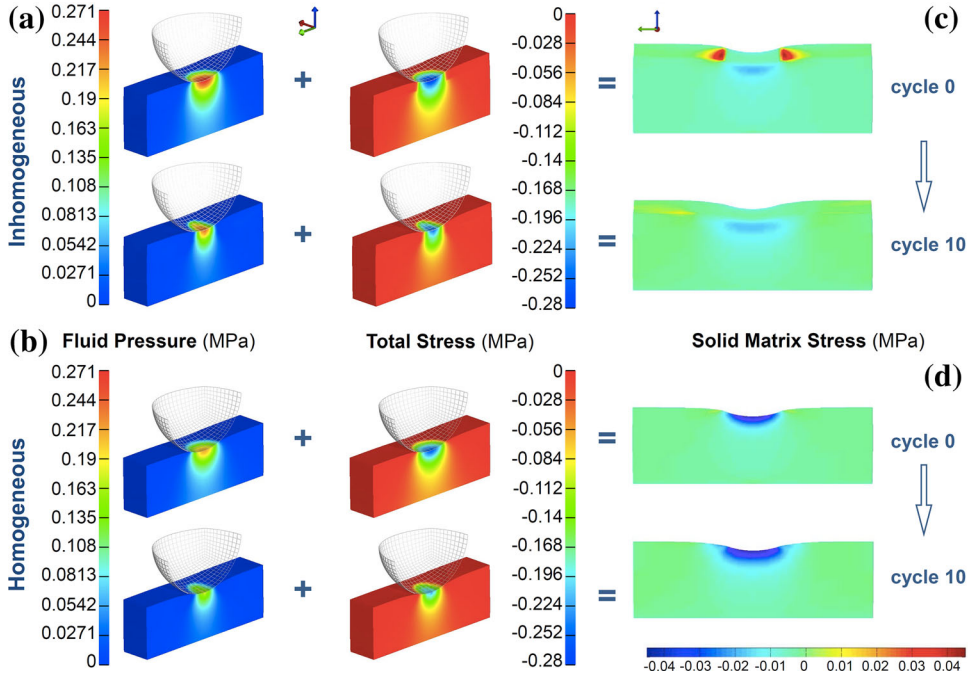

FIGURE 5. Interstitial fluid pressure and stress during probe sliding as predicted by FE simulation. Fluid pressure and total stress (principal normal stress) are reported in the (a) heterogeneous and (b) homogeneous models within the cartilage immediately after compressive loading (top) and following 10 sliding cycles (bottom). Both fluid pressure and total stress decreased after 10 cycles of sliding. The stress field in the solid matrix for (c) heterogeneous and (d) homogeneous models can be calculated as the sum of the corresponding fluid pressure and total stress. The heterogeneous model, consisting of both the superficial and the middle-deep zones, shows lower solid matrix stress after 10 sliding cycles, which leads to a lower friction coefficient.

with the superficial zone (Fig. 5c) compared to without (Fig. 5d).

To quantify the contribution of fluid pressure during sliding, the fluid load support ratio is plotted over time (Fig. 6). At the initiation of sliding, immediately following 10% compression, the fluid load support ratio is 98.5% in the heterogeneous model and merely 85.1% in the homogeneous model (Fig. 6a). A simple calculation indicates that the mechanical loading supported by the solid matrix in the homogeneous case is 7.5 times higher than that in the heterogeneous model (15 vs. 2%), which implies much higher friction as the friction force is mainly generated by solid–solid contact. During the 10 sliding cycles, the fluid load support ratio decreases but remains above 92% in the heterogeneous model, while precipitously diminishing to 60% in the homogeneous tissue. Furthermore, loss of the superficial layer accelerates the temporal decrease of IFP during continuous sliding. At the end of 10 cycles, the fluid load support ratio is higher at 2 mm/s speed than 1 mm/s in both models, while the decline of the fluid support with sliding is more significant in the homogeneous model (heterogeneous: 95.2 vs. 92.6%; homogeneous: 73.7 vs. 60.6%). Moreover, the fluid load support ratio in the heterogeneous model is virtually insensitive to variation in normal loading magnitude. The fluid load support ratio after 10 sliding cycles is almost identical for 10% ($W_p/W = 92.6\%$) and 15% ($W_p/W = 92.7\%$) compressive strains (Fig. 6b). In contrast, the 10% compressive strain level in the homogeneous model displays a markedly lower fluid load support ratio than the 15% strain level, from the initiation of sliding to the end of the 10th cycle (initial: 85.0 vs. 88.0%; end: 60.6 vs. 67.3%). The rates of fluid pressure decrease are similar under the two loading levels, in contrast to the marked difference displayed under the two sliding speeds.

As the presence of the superficial zone promotes IFP inside the tissue, the distinct mechanical properties and sharp transition between the two layers could generate high shear stress at the interface, a hypothesis confirmed by FE simulations. A concentration of shear stress in the heterogeneous model is revealed at the interface between the superficial and middle-deep zones, particularly for the tissue underneath the probe-cartilage contact area (Fig. 7a); such shear is not present in the homogeneous model (Fig. 7b). This high shear force requires a robust binding structure at the interface to avoid the tearing of the top layer. The rooting of large collagen bundles from the fibrous zone into the middle-deep zone cartilage provides such a

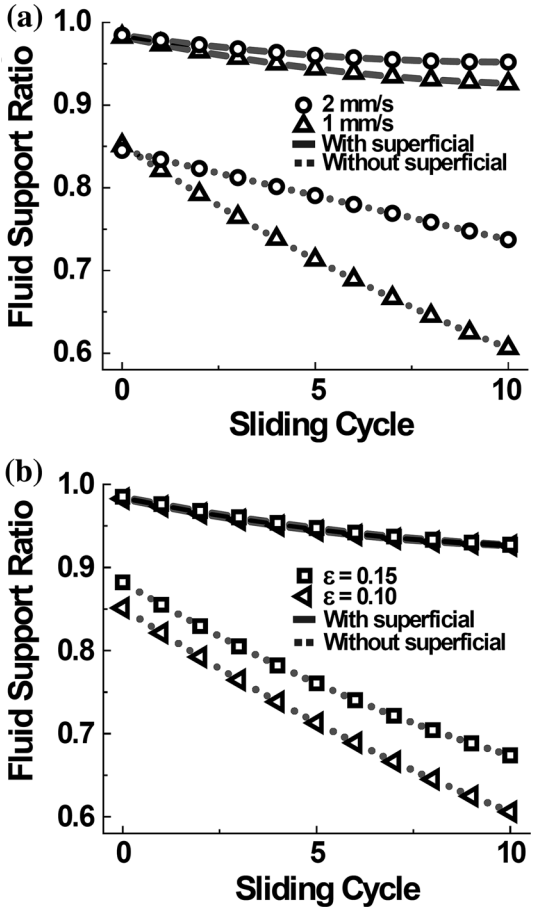

FIGURE 6. Fluid load support ratio in TMJ condylar cartilage during sliding. (a) Fluid load support ratio with and without superficial zone, at 1 and 2 mm/s sliding speeds (normal strain = 10%). Fluid load support ratio in the heterogeneous model is significantly elevated with a heightened ability to maintain fluid pressurization over time when compared to the homogeneous model. In the absence of the superficial layer, the fast sliding speed (2 mm/s) generates greater fluid pressurization than the slow speed (1 mm/s). (b) Fluid load support ratio with and without the superficial zone, at 10 and 15% normal strain (sliding speed = 1 mm/s). For the heterogeneous model, changing compressive strain has little effect on the fluid load support ratio over time. In the homogeneous model, higher strain provides higher fluid load support.

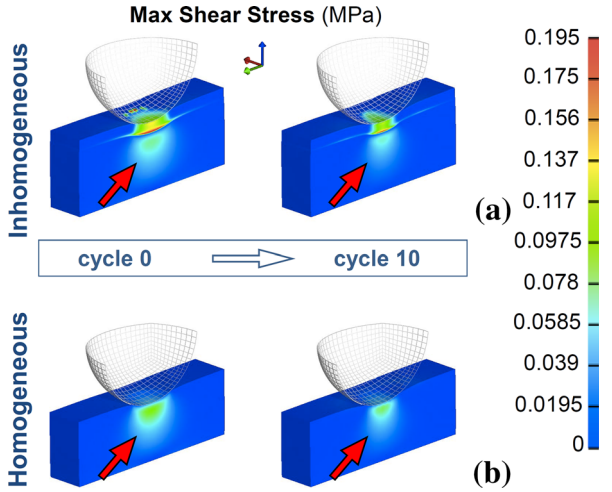

FIGURE 7. Shear stress ($\tau_{xy,max}$) in TMJ condylar cartilage. Maximum shear stress in the (a) heterogeneous and (b) homogeneous model before the initiation of sliding and after completion of 10 sliding cycles. A concentration of shear stress exists at the interface between the two zones in the heterogeneous model.

binding structure with the necessary strength to resist the high shear generated during motion.

DISCUSSION

Heterogeneous and Nonlinear Mechanical Properties

Mechanical testing in this study disclosed a stark disparity between the mechanical properties of the two zones. The tensile modulus of the superficial zone, as measured in the dominant fiber direction, is significantly higher than that of the middle-deep zone. The result for the superficial zone is in excellent agreement with those from a dedicated study,[36] which reported a tensile modulus of 29 ± 13 MPa for the central region of porcine TMJ condylar cartilage in the AP direction (comparable to our tests). Since the tensile modulus of the superficial zone in normal hyaline cartilage ranges from 5 to 20 MPa and typically falls in the lower end,[1,22,39,46] it is clear the superficial zone of TMJ condylar cartilage displays a higher tensile modulus than that of normal hyaline cartilage. This matches the composition and ultrastructure of the superficial zone in TMJ condylar cartilage, which contains aligned type I collagen bundles similar to ligament or tendon tissues. The tensile modulus of the middle-deep zones in normal hyaline cartilage generally ranges between 0.9 and 9 MPa.[1,22] The tensile modulus of the middle-deep zone in TMJ condylar cartilage falls in this range, although the TMJ cartilage is uniquely interdigitated with type I collagen bundles.

For typical hyaline cartilage, Schinagl *et al.*[35] reported that the superficial layer has a compressive modulus of 0.079 MPa, increasing to 0.7 MPa for the middle-deep zone, whereas Krishnan *et al.* gave values of ~0.30 and 0.73 MPa for the two zones, respectively.[22] In this study, the compressive modulus also increases with depth in TMJ condylar cartilage, from 0.028 MPa in the superficial zone to 0.14 MPa in the middle-deep zone. The high compressive modulus of the middle-deep zone allows the tissue to support compressive loading with minimal deformation, consequently reducing the contact area on the condylar surface during sliding. As a small contact area is essential to reduce plowing and frictional forces in a sliding (or MCA) modality,[31] such heterogeneity and

nonlinearity in TMJ condylar cartilage implies that the superficial zone serves primarily to transmit and support tensile loading whereas the middle-deep zone provides resistance to compressive loading, supporting a previous hypothesis of the different mechanical roles for each layer.[37]

Although the middle-deep zone of TMJ condylar cartilage is similar to hyaline cartilage, it is interdigitated with vertical type I collagen bundles. Little knowledge is available about the biomechanical functions of this unique ultrastructure. As the fibers are aligned mainly in the vertical direction and offer no resistance to buckling, they should provide little contribution to the tissue's ability to resist compressive loading. When the tissue is under compression, the tensile stress is mainly in the radial direction. Thus the vertical fibers are not arranged to resist tissue expansion either. Our FE simulation, for the first time, revealed the existence of a high shear force at the interface between the superficial and middle-deep layers, which arises naturally due to the different properties of the two layers and the abrupt transition at the interface. The vertical type I collagen fibers traversing the two layers can efficiently resist this shear stress and prevent detaching of the two layers, which may represent one of the mechanical functions of this unique ultrastructure in TMJ condylar cartilage.

Effects of Heterogeneity and Nonlinearity on IFP

Previous work has demonstrated that tension–compression nonlinearity of the solid matrix contributes essentially to the interstitial fluid pressurization in loaded hyaline cartilage, as the high tensile stiffness causes a great resistance to tissue expansion under compressive loading.[32,39] In hyaline cartilage, the top 10–20% of tissue is usually considered as the "superficial tangential" zone, in which the type II collagen fibrils are mainly aligned in a plane parallel to the cartilage-bone interface. It was found that the peak fluid support ratio is higher at the articular surface of the tissue than at the deep zone, because the disparity between the tensile and compressive moduli is greater at the surface due to unified alignment of collagen. In this study, the tensile to compressive moduli ratio in the superficial zone of condylar cartilage is extremely large (1098:1), approaching the values of fibrous tissues such as tendons,[47] while the ratio in the middle-deep zone is 17.4:1, similar to the deep zone in hyaline cartilage.[32] For comparison, the ratio was reported as 36:1 in the superficial zone and 9.4:1 in the deep zone of patellar cartilage, and 67:1 in the superficial zone and 8.5:1 in the deep zone of femoral cartilage.[32] Previous studies on hyaline cartilage proved that the depth-dependent inhomogeneity of the material properties, especially the presence of the tension–compression nonlinear superficial zone, promotes IFP at the articular surface, and the interstitial fluid support in knee cartilage can reach 97–98%.[2,22,32] Therefore, the superficial fibrous layer of TMJ condylar cartilage and its tension–compression nonlinearity should be able to significantly boost interstitial fluid pressurization during loading. Our FE simulations predicted that IFP supports 98.5% of the load on TMJ condylar cartilage under 10% compressive deformation and 2 mm/s sliding speed (Fig. 6a). In the same conditions for condylar cartilage without the superficial zone (homogeneous model), the FE simulation predicts a reduction in IFP load support to 85.1%, i.e., the load supported by the solid phase increased by an order of magnitude without the superficial layer (1.5 vs. 14.9%). Additionally, the heterogeneous structure slowed the depletion of fluid pressurization compared to the homogeneous model. The fluid load support ratio can be maintained at over 95% after 10 sliding cycles (15 s) (Fig. 6a). These results strongly suggest that the tissue heterogeneity confers a unique nonlinear mechanical behavior to TMJ condylar cartilage, representing a functional adaptation to maximize IFP-related lubrication at the cartilage surface.

Effects of Sliding Speed and Load on Frictional Coefficient

An increase in sliding speed from 1 to 2 mm/s enhances the fluid load support ratio (Fig. 6a), supporting our experimental results showing a decrease in friction coefficient with increasing sliding speed (Fig. 2b).[9,14,27] Under MCA testing, higher sliding speed means less time in contact and, therefore, less exudation with each cycle up to an asymptotic limit when $Pe \gg 1$.[7] Since 2 mm/s sliding speed is on the low end of physiological values,[13] the fluid load support ratio in TMJ condylar cartilage during daily functions could be maintained at a very high value as predicted by our FE simulation. In the heterogeneous model, the fluid load support ratio remained virtually identical at strain levels of 10 and 15% (Fig. 6b), consistent with the experimental results that showed no correlation between friction coefficient and loading magnitude (Fig. 2c). In contrast, the homogeneous model displayed increased fluid load support with increased loading, which may be partially due to the lower permeability under larger strain. However, such effects are minimized in the heterogeneous model due to the extreme stiffening effect provided by the surface collagen fibers, which resist lateral deformation and therefore strive to maintain minimal deformation under high loading.

Limitations

A number of limitations in this study should be noted. Firstly, IFP plays an essential role in regulating the frictional response of cartilage, but is not the only factor. Hydrodynamic, elastohydrodynamic, boosted,[11,45] and squeeze film[11] mechanisms, plowing forces, and boundary lubrication[14,16] may each have affected the friction measurements. Therefore, it is important to note that the present study only revealed how the fibrous zone affects IFP and further the biphasic lubrication of condylar cartilage. The existence of the fibrous layer may also regulate the lubrication through other mechanisms. Secondly, in our MCA frictional tests, the sliding speed and normal loading only cover limited ranges, in which the Peclet numbers are $\gg 1$, i.e., IFP remains the dominant lubrication mechanism. This contributes to the consistency between the trends revealed by frictional tests and FE simulation. The effects of IFP on lubrication disclosed in this study may change or vanish under different loading regimes, such as stationary contact sliding. Furthermore, it is likely that testing in synovial fluid, rather than PBS, may result in slightly lower friction coefficients due to boundary lubrication, although the trends reported here would remain preserved.[9] Thirdly, the comprehensive FE model is still a simplification of the actual ultrastructure of the tissue. For example, the fiber reinforced model for the middle-deep zone only addressed the type II collagen fibers in the solid matrix, but not the vertical type I collagen fibers originating from the superficial zone. Additionally, the solid matrix was assumed to be isotropic, while both the superficial layer and middle-deep zone are highly anisotropic in structure. Fourthly, frictionless contact was assumed between the indenter and cartilage in the FE simulation. Incorporation of a friction force at the migrating interface of porous-elastic media remains a critical challenge in modeling and simulation. For the simulated regime in this study, the friction force should be small and have limited influence on the predicted IFP in cartilage. Furthermore, in this study the reported statistical calculations do not combine data from the same animal and report the number of animals as N, although it has been suggested that this procedure provides a more rigorous analysis.[34] In light of this, the data was reexamined and it was found that the paired analysis did not add or remove any significance from the results. Finally, the limited power of modern computers obviates the simulation of all possible loading regimes. For example, more than 3 weeks' computing time is required for a modern workstation (equipped with dual Intel Xeon Processors, 12 cores at 2.8 GHz, 64 GB memory) to simulate 10 sliding cycles at 0.1 mm/s. Thus only necessary simulations were performed to reveal the general trend of IFP over sliding speeds, loading magnitudes, and tissue heterogeneity.

ACKNOWLEDGMENTS

The authors would like to thank Dr. Dawn Elliott for assistance in the measurement of tissue cross-sectional area and Dr. Gerard Ateshian for assistance with FEBio modeling.

CONFLICT OF INTEREST

All authors state that they have no conflicts of interest.

REFERENCES

[1]Akizuki, S., *et al.* Tensile properties of human knee joint cartilage: I. Influence of ionic conditions, weight bearing, and fibrillation on the tensile modulus. *J. Orthop. Res.* 4(4):379–392, 1986.
[2]Ateshian, G. A. The role of interstitial fluid pressurization in articular cartilage lubrication. *J. Biomech.* 42(9):1163–1176, 2009.
[3]Ateshian, G. A., S. Maas, and J. A. Weiss. Finite element algorithm for frictionless contact of porous permeable media under finite deformation and sliding. *J. Biomech. Eng.* 132(6):061006, 2010.
[4]Ateshian, G. A., *et al.* Modeling the matrix of articular cartilage using a continuous fiber angular distribution predicts many observed phenomena. *J. Biomech. Eng.* 131(6):061003, 2009.
[5]Bermejo, A., O. Gonzalez, and J. M. Gonzalez. The pig as an animal model for experimentation on the temporomandibular articular complex. *Oral Surg. Oral Med. Oral Pathol.* 75(1):18–23, 1993.
[6]Bonnevie, E. D., *et al.* In-situ studies of cartilage microtribology: roles of speed and contact area. *Tribol. Lett.* 41(1):83–95, 2011.
[7]Bonnevie, E. D., *et al.* Fluid load support during localized indentation of cartilage with a spherical probe. *J. Biomech.* 45(6):1036–1041, 2012.
[8]Burris, D. L., and W. G. Sawyer. Addressing practical challenges of low friction coefficient measurements. *Tribol. Lett.* 35(1):17–23, 2009.
[9]Caligaris, M., and G. A. Ateshian. Effects of sustained interstitial fluid pressurization under migrating contact area, and boundary lubrication by synovial fluid, on cartilage friction. *Osteoarthr. Cartil.* 16(10):1220–1227, 2008.
[10]Detamore, M. S., and K. A. Athanasiou. Tensile properties of the porcine temporomandibular joint disc. *J. Biomech. Eng.* 125(4):558–565, 2003.
[11]Dowson, D., V. Wright, and M. D. Longfield. Human joint lubrication. *Biomed. Eng.* 4(4):160–165, 1969.
[12]Forster, H., and J. Fisher. The influence of loading time and lubricant on the friction of articular cartilage. *Proc. Inst. Mech. Eng. H* 210(2):109–119, 1996.

[13]Gallo, L. M., *et al*. Stress-field translation in the healthy human temporomandibular joint. *J. Dent. Res*. 79(10): 1740–1746, 2000.
[14]Gleghorn, J. P., and L. J. Bonassar. Lubrication mode analysis of articular cartilage using Stribeck surfaces. *J. Biomech*. 41(9):1910–1918, 2008.
[15]Gleghorn, J. P., *et al*. Alteration of articular cartilage frictional properties by transforming growth factor beta, interleukin-1beta, and oncostatin M. *Arthritis Rheum*. 60(2):440–449, 2009.
[16]Gleghorn, J. P., *et al*. Boundary mode lubrication of articular cartilage by recombinant human lubricin. *J. Orthop. Res*. 27(6):771–777, 2009.
[17]Holmes, M. H., and V. C. Mow. The nonlinear characteristics of soft gels and hydrated connective tissues in ultrafiltration. *J. Biomech*. 23(11):1145–1156, 1990.
[18]Huang, C. Y., *et al*. Anisotropy, inhomogeneity, and tension-compression nonlinearity of human glenohumeral cartilage in finite deformation. *J. Biomech*. 38(4):799–809, 2005.
[19]Ingawale, S., and T. Goswami. Temporomandibular joint: disorders, treatments, and biomechanics. *Ann. Biomed. Eng*. 37(5):976–996, 2009.
[20]Katta, J., *et al*. Biotribology of articular cartilage—a review of the recent advances. *Med. Eng. Phys*. 30(10):1349–1363, 2008.
[21]Krishnan, R., M. Kopacz, and G. A. Ateshian. Experimental verification of the role of interstitial fluid pressurization in cartilage lubrication. *J. Orthop. Res*. 22(3):565–570, 2004.
[22]Krishnan, R., *et al*. Inhomogeneous cartilage properties enhance superficial interstitial fluid support and frictional properties, but do not provide a homogeneous state of stress. *J. Biomech. Eng*. 125(5):569–577, 2003.
[23]Lewis, P. R., and C. W. McCutchen. Experimental evidence for weeping lubrication in mammalian joints. *Nature* 184:1285, 1959.
[24]Lu, X. L., V. C. Mow, and X. E. Guo. Proteoglycans and mechanical behavior of condylar cartilage. *J. Dent. Res*. 88(3):244–248, 2009.
[25]Lu, X. L., *et al*. Indentation determined mechanoelectrochemical properties and fixed charge density of articular cartilage. *Ann. Biomed. Eng*. 32(3):370–379, 2004.
[26]Maas, S. A., *et al*. FEBio: finite elements for biomechanics. *J. Biomech. Eng*. 134(1):011005, 2012.
[27]Moore, A. C., and D. L. Burris. An analytical model to predict interstitial lubrication of cartilage in migrating contact areas. *J. Biomech*. 47(1):148–153, 2014.
[28]Mow, V. C., W. Y. Gu, and F. H. Chen. Structure and function of articular cartilage and meniscus. In: Basic Orthopaedic Biomechanics and Mechano-Biology, edited by V. C. Mow, and R. Huiskes. Philadelphia: Lippincott Williams & Wilkins, 2005, pp. 181–258.
[29]Mow, V. C., *et al*. Biphasic indentation of articular cartilage—II. A numerical algorithm and an experimental study. *J. Biomech*. 22(8–9):853–861, 1989.
[30]Murphy, M. K., *et al*. Temporomandibular disorders: a review of etiology, clinical management, and tissue engineering strategies. *Int. J. Oral Maxillofac. Implants* 28(6):e393–e414, 2013.
[31]Nickel, J. C., *et al*. Tractional forces on porcine temporomandibular joint discs. *J. Dent. Res*. 88(8):736–740, 2009.
[32]Park, S., *et al*. Cartilage interstitial fluid load support in unconfined compression. *J. Biomech*. 36(12):1785–1796, 2003.
[33]Pawaskar, S. S., J. Fisher, and Z. Jin. Robust and general method for determining surface fluid flow boundary conditions in articular cartilage contact mechanics modeling. *J. Biomech. Eng*. 132(3):031001, 2010.
[34]Ranstam, J. Repeated measurements, bilateral observations and pseudoreplicates, why does it matter? *Osteoarthr. Cartil*. 20(6):473–475, 2012.
[35]Schinagl, R. M., *et al*. Depth-dependent confined compression modulus of full-thickness bovine articular cartilage. *J. Orthop. Res*. 15(4):499–506, 1997.
[36]Singh, M., and M. S. Detamore. Tensile properties of the mandibular condylar cartilage. *J. Biomech. Eng*. 130(1): 011009, 2008.
[37]Singh, M., and M. S. Detamore. Biomechanical properties of the mandibular condylar cartilage and their relevance to the TMJ disc. *J. Biomech*. 42(4):405–417, 2009.
[38]Soltz, M. A., and G. A. Ateshian. Experimental verification and theoretical prediction of cartilage interstitial fluid pressurization at an impermeable contact interface in confined compression. *J. Biomech*. 31(10):927–934, 1998.
[39]Soltz, M. A., and G. A. Ateshian. A conewise linear elasticity mixture model for the analysis of tension–compression nonlinearity in articular cartilage. *J. Biomech. Eng*. 122(6):576–586, 2000.
[40]Spilker, R. L., J. C. Nickel, and L. R. Iwasaki. A biphasic finite element model of in vitro plowing tests of the temporomandibular joint disc. *Ann. Biomed. Eng*. 37(6):1152–1164, 2009.
[41]Szczesny, S. E., *et al*. Biaxial tensile testing and constitutive modeling of human supraspinatus tendon. *J. Biomech. Eng*. 134(2):021004, 2012.
[42]Tanaka, E., *et al*. The frictional coefficient of the temporomandibular joint and its dependency on the magnitude and duration of joint loading. *J. Dent. Res*. 83(5):404–407, 2004.
[43]Tanaka, E., *et al*. The effect of removal of the disc on the friction in the temporomandibular joint. *J. Oral Maxillofac. Surg*. 64(8):1221–1224, 2006.
[44]Tanaka, E., *et al*. Lubrication of the temporomandibular joint. *Ann. Biomed. Eng*. 36(1):14–29, 2008.
[45]Walker, P. S., *et al*. "Boosted lubrication" in synovial joints by fluid entrapment and enrichment. *Ann. Rheum. Dis*. 27(6):512–520, 1968.
[46]Williamson, A. K., *et al*. Tensile mechanical properties of bovine articular cartilage: variations with growth and relationships to collagen network components. *J. Orthop. Res*. 21(5):872–880, 2003.
[47]Yin, L., and D. M. Elliott. A biphasic and transversely isotropic mechanical model for tendon: application to mouse tail fascicles in uniaxial tension. *J. Biomech*. 37(6):907–916, 2004.
[48]Zimmerman, B. K., *et al*. Role of interstitial fluid pressurization in TMJ lubrication. *J. Dent. Res*. 94(1):85–92, 2015.